Hybrid BTMS for Lithium-Ion Batteries

Chakib Alaoui*, Mhamed Zineddine
INSA Euro-Méditerranée
Euromed University
Fès, Morocco
c.alaoui@insa.ueuromed.org
m.zineddine@insa.ueuromed.org

Mohammed Boulmalf
International University of Rabat
Rabat, Morocco
mohammed.boulmalf@uir.ac.ma

Abstract – **Lithium-ion (li-ion) batteries are considered as the best choice available for energy storage system (EES) for portable devices, electric and hybrid vehicles and smart grid, thanks to their high energy and power densities, lack of memory effect and life cycle. However, the heat generated by these batteries remains a challenge. Without an appropriate battery thermal management system (BTMS), the li-ion battery surface temperature can increase very quickly, and thus creating a hazard for the users and the equipment. This paper presents a solid-state hybrid active/passive BTMS system. It includes Peltier effect heat pumps, heat sinks, heat spreaders and fans. It is designed with the objective of regulating the operating temperature of the battery cells while minimizing the parasitic power used to operate the BTMS. After its construction, C/1, 3C and 5C continuous discharge current tests were applied under ambient temperature values of –20°C, 0°C, 25°C and 40°C. Experimental results show that the proposed hybrid BTMS works in passive mode (hence does not consume any power) in an ambient temperature ranging from 0°C to 25°C, and consumes very little power in extreme values (less than 5% of available stored energy in li-ion battery pack).**

Keywords-component; lithium-ion battery; battery thermal management system; Peltier thermoelectric module;

I. INTRODUCTION

Lithium-ion (li-ion) batteries are considered as the best choice available for energy storage system (EES) for portable devices, electric and hybrid vehicles and smart grid, thanks to their high energy and power densities, lack of memory effect and life cycle [1]. However, the heat generated by these batteries remains a challenging task, as active BTMS consume too much energy from the battery pack, add weight to the vehicle, and thus reducing the range of the vehicle. On the other hand, without an appropriate battery thermal management system (BTMS) that actively cools down the li-ion cells, their surface temperature increases rapidly [2]. High temperature values have a detrimental effect on the batteries as their cycle life diminishes [3-5]. Their surface temperature can easily exceed 50°C and approach the temperature limits, and thus producing a hazard for the vehicle and its occupants with a high risk of thermal run-away, gassing and even explosion [6-8]. In order to design a suitable BTMS, the heat generated by a prismatic li-ion battery pack was quantified [9]. The results obtained were used to attune Peltier effect thermoelectric devices (TEDs) along with heat-spreaders, heat-sinks and fans. Since the BTMS consumes power from the li-ion battery pack (referred to as parasitic power) and it is mounted on board of the vehicle, it should consume the minimal amount of parasitic power, occupy the minimum space and have the lowest weight in order not to affect the range and performance of the vehicle.

This paper presents a solid-state hybrid active/passive cooling system that cools the li-ion battery pack according to two modes of operations:

1. "Passive mode", in which the BTMS consumes enough power from the battery pack to run only the fans.
2. "Active mode", in which the BTMS draws power to feed the Peltier solid-states heat pumps and the fans.

A control circuit selects the appropriate mode of operation according to the surface temperature of the batteries. This paper is organized as follows. First the thermal profile of the li-ion battery cell is evaluated in section II. Section III presents an overview of the Peltier effect solid-state cooling principles and the design of the proposed BTMS. Section IV and V shows some experimental results validating the feasibility of this system. This paper ends with a conclusion in section VI.

II. THERMAL PROFILE OF LI-ION BATTERY

A. Energy balance

The maximum value of the energy that can be saved on an electrochemical battery or drawn from it depends on the change in Gibbs energy [10]. During both the charging and the discharging of a battery system, there are losses due to the internal resistance of the battery, activation polarization that activates the electrochemical reaction at the electrode surface and concentration polarization. These losses generate heat that must be evaluated in order to design a proper BTMS [11]. The amount of heat generated by an electrochemical cell is usually expressed by an equation referred to as Bernardi's energy balance [12], in which a heat loss in a battery cell is expressed in (1).

$$Q = I\left(U_{ocv} - U_{bat} - T\,\partial U_{ocv}/\partial T\right) \qquad (1)$$

Where I is the current (A), U_{ocv} is the open-circuit voltage (V), U_{bat} is the battery voltage (V), and T is the temperature of the battery (K). The first term of (1) is referred to as the

978-1-5386-2847-8/17/$31.00 ©2017 IEEE

irreversible portion of the heat loss and is caused by the Joule heating. It is proportional to the cell's internal resistance and the square of the current ($R_{int}I^2$), the second portion is referred to as the reversible heat loss and is caused by the entropy related thermal energy. It is possible to evaluate the total losses by using the "energy method" [13]. This method is about establishing the energy balance during charge and discharge, and then evaluating the difference.

When charging the battery from an initial state of charge SOC_1 to a final state of charge SOC_2, the required energy is E_{Char}, expressed in (2):

$$E_{Char} = E_{BATT} + E_{Char,rev} + E_{Char,irrev} \quad (2)$$

Where E_{BATT} is the energy stored in the battery, $E_{char,rev}$ is the energy corresponding to the entropy change, and $E_{Char,irrev}$ is the energy dissipated by polarization. Similarly, when discharging the battery from SOC_2 back to SOC_1, the total energy is expressed in (3)

$$E_{BATT} = E_{Disch} + E_{Disch,rev} + E_{Disch,irrev} \quad (3)$$

Where E_{Disch} is the electrical work performed by the battery, $E_{Disch,irrev}$ is the energy corresponding to the entropy change and $E_{Disch,irrev}$ is the energy dissipation by polarization. Finally, the total energy lost during the cycle is in (4)

$$E_{LOSSES} = \left(E_{Char,rev} + E_{Disch,rev}\right) + \left(E_{Char,irrev} + E_{Disch,irrev}\right) \quad (4)$$

And the total heat loss is expressed in equation (5)

$$Q_{BATT} = E_{LOSSES} / \Delta t \quad (5)$$

Where Δt is the time interval required to go from SOC_1 to SOC_2. At a high current rate, the contribution of irreversible heat (i.e., polarization resistance heat and ohmic resistance heat and tab resistance) becomes dominant, the total heat lost largely depends on the value of the lumped internal resistance R_{int} that encompasses the resistivity of the components of the battery. R_{int} is further influenced by material contacts (e.g., between active material and the current collector), geometrical electrode (thickness, dimensions) and internal construction aspects.

B. Heat generation test

Energy balance equation is used to evaluate the heat loss as in [13]. In order to charge the battery cell, the recommended constant current / constant voltage method was applied. A constant current of C/1 = 20A is applied until the voltage limit (3.6 V) is reached. This is followed by the application of a constant voltage (3.6 V) while having an exponential decrease of the applied current. The charge process is terminated when the current reaches 0.02C. E_{Char} is then evaluated. Concerning the discharge, the 20AH li-ion cell was discharged at discharge rates of C/1 and 5C continuous current. The charge/discharge procedure was repeated at different value of ambient temperature (–20 ºC, 0 ºC, 24 ºC and 40 ºC) by putting the battery cell inside a climatic chamber of type Espec LHU 112M-U. It has a range of temperature values of –20 °C to 85 °C with a precision of ±0.5 °C. Table I shows some specifications of the 20 AH lithium iron phosphate ($LiFePO_4$) cell used in this experiment.

TABLE I. LI-ION CELL SPECIFICATIONS

Specification	**Value**
Nominal capacity (Ah)	19.5
Nominal discharge power (W)	1200
Voltage range (V)	2 – 3.6
Recommended maximum charge current (A)	100
Operating temperature (°C)	-30 to 55
Recommended temperature (°C)	0 to 40

The first test was a full cycle run at an ambient temperature of –20 °C. The charge was of a constant current-constant voltage method with a total energy input to the battery of E_{Char} = 59 Wh. A discharge at C/1 rate gave E_{Disch} = 45.1 Wh, thus making a loss of 13.9 Wh. The average heat rate produced by the li-ion cell is found to be 17.7 W having the discharge running for Δt = 47min. Finally, the efficiency is calculated to be η = 76.44%.The same experiment was repeated for 5C discharge rate and for –20 °C, 0 °C, 25 °C and 40 °C. Table II shows the experimental results, and Fig. 1 and Fig. 2 and table II show the C/1 and 5C discharge tests. The maximum value of the heat generated form the li-ion cell was 104.5 W corresponding to a discharge of a continuous current of 5C (100 A) and an ambient temperature of –20 °C. The proposed BTMS is designed to accommodate 24 li-ion cells, hence a total of 2508 W of heat need to be removed (this amount of heat is generated under extreme conditions).

TABLE II. HEAT GENERATION RATE MEASUREMENTS

T_∞ (°C)	η (%)	E_{Char} (Wh)	E_{Disch} (Wh)	E_{Loss}	Q_{BATT}
C/1 Discharge test					
–20	76.56	59	45.1	13.9	17.75
0	82.27	62	51	11	12.7
24	95.1	65	61.82	3.18	3.23
40	98.3	66	64.88	1.12	1.12
5C Discharge test					
–20	73.45	59	43.34	15.66	104.5
0	80.75	62	50.07	11.93	59.53
24	90.38	65	58.75	6.25	27.05
40	94.15	66	62.14	3.86	14.3

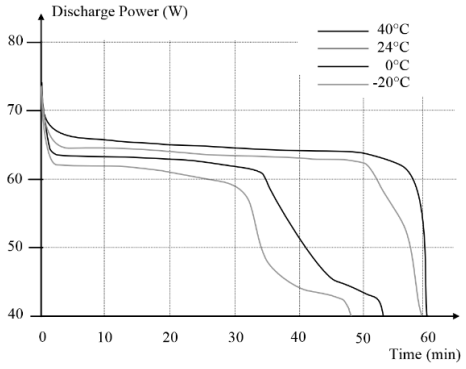

Fig. 1. C/1 discharge test

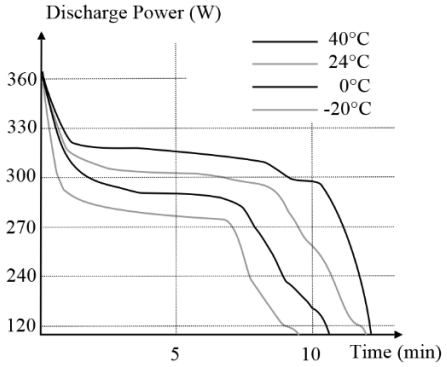

Fig. 2. 5C discharge test

III. BTMS Design and Modeling

A. Peltier cooling principles

A TED consists of a number of semiconductor thermocouples sandwiched between two layers of ceramic substrates. Active heat removal is achieved with the application of DC current through a series of thermocouple 'legs' that are electrically connected in series and thermally in parallel. As the excess electrons move from the p type material to the n type material, the electrons jump to a higher energy state absorbing thermal energy. TEDs are used in electronics, instrumentation and biotechnology related applications [14-21]. Fig. 3 shows the principle of Peltier cooling.

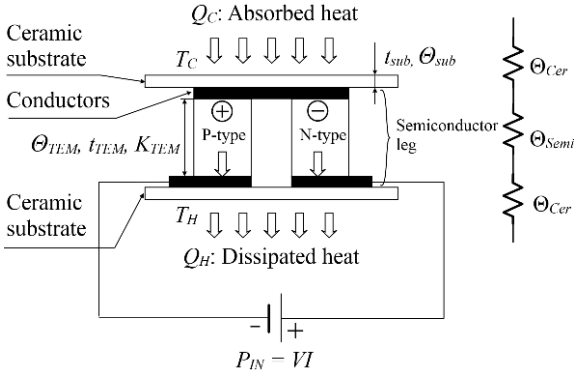

Fig. 3. Physical representation of a leg of a TED

The heat absorbed Q_C and dissipated Q_H by a TED is expressed by (6) and (7), where ΔT is the temperature difference between the hot and the cold side of the device $\Delta T = T_H - T_C$. R, α and K are the electrical resistance and the Seebeck thermal conductance respectively. n is the number of pairs of thermoelectric legs in the device.

$$Q_C = 2n\left(\alpha I T_C - \frac{1}{2}RI^2 - K.\Delta T\right) \quad (6)$$

$$Q_H = 2n\left(\alpha I T_C + \frac{1}{2}RI^2 - K.\Delta T\right) \quad (7)$$

In section II, it was found that the 20Ah li-ion cell generated 104.5 W of heat under 5C discharge current and –20 °C ambient temperature. For a total of 24 cell, the total amount of heat would be 2508 W. In order to remove it from the li-ion battery pack, a high power Peltier cooling module from Ferrotec was selected (9501/242/160B). Table III shows the properties of the device, with T_m being the average temperature from inlet to the outlet of the hot and cold sides of the Peltier device.

TABLE III. 9501/242/160B TED SPECIFICATIONS [22]

Symbol	Description	Value
	TED dimension (mm^3)	55 x 55 x 3.45
n	Number of pair of legs per TED	242
V	Maximal voltage (V)	33.3
I	Maximal current (A)	16
Q_c	Maximal thermal power (W)	289
ΔT	Maximal temperature difference (°C)	72
α	Seebeck coefficient (V/K)	0.201
R_{elec}	Electrical resistance (Ω)	1.7352

TED is constructed by inserting n semiconductor legs between two ceramic substrates as shown in Fig. 3. The thermal resistance of N TEDs is Θ_{TED}, when no power is applied, is the series connection of the thermal resistance of the ceramic substrate Θ_{Cer} and the semiconductor legs Θ_{Semi} (the thermal resistance of the connecting conductors is ignored). The thermal resistances are expressed in (10), (11) and (12).

$$\Theta_{Cer} = \frac{t_{Cer}}{n.K_{Cer}.A_{Cer}} \quad (10)$$

$$\Theta_{Semi} = \frac{t_{semi}}{K_{Semi}(2.n.N.A_{Semi})} \quad (11)$$

$$\Theta_{TED} = 2\Theta_{Cer} + \Theta_{Semi} \quad (12)$$

With t_{Cer}, K_{Cer}, A_{Cer}, t_{Semi}, K_{Semi} and A_{Semi} are the thickness, the thermal conductivity and the cross-sectional area of the ceramic substrate and of the semiconductor leg respectively.

B. BTMS physical design

The heat spreader was designed to accommodate the 20 Ah li-ion cell with geometry shown in Fig. 4. It fulfills the following specifications:

1. It must mechanically support 24 li-ion cells. A pair of cells are stacked between the fins of the heat spreader as shown in Fig.s 5 and 6. In order to maintain a pressure under 10 psi between the surface of the prismatic cell and the surface of the heat spreader, a thin layer of fire retardant neoprene was put between two li-ion cells. This is done in order to reduce swelling that damages the internal structure of the li-ion cell, affecting its state of charge (SOC) and state of health (SOH) [23]. In addition, it aids in damping the vibrations within the BTMS while the vehicle moves, while maintaining an even pressure distribution between the li-ion cells.
2. It must transfer the heat generated by the li-ion batteries to the TEDs and heat sinks in order to maintain the cell's temperature within the recommended limits. The model proposed in Fig. 7 is used to evaluate the thermal resistance of the heat spreader.

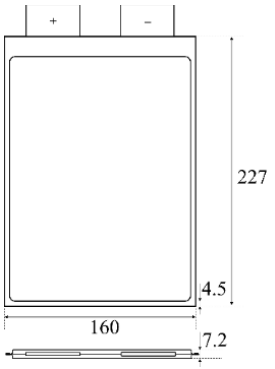

Fig. 4. 20 Ah $LiFePO_4$ prismatic pouch cell dimensions.

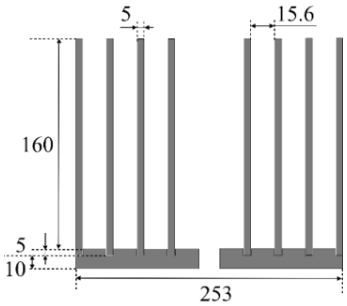

Fig. 5. Heat spreader and support for li-ion cells for BTMS

Twelve TEDs of reference 9501/242/160B [22] are mounted on the base of the heat spreader in order to remove the heat Q_{BATT} produced by the li-ion battery cells as shown in Fig. 6. Finally, a heat sinks and fans (NF-A14 PWM – 140x140x25mm^3 / 3000 RPM) are mounted on the other side of the TEDs as shows in Fig. 6.

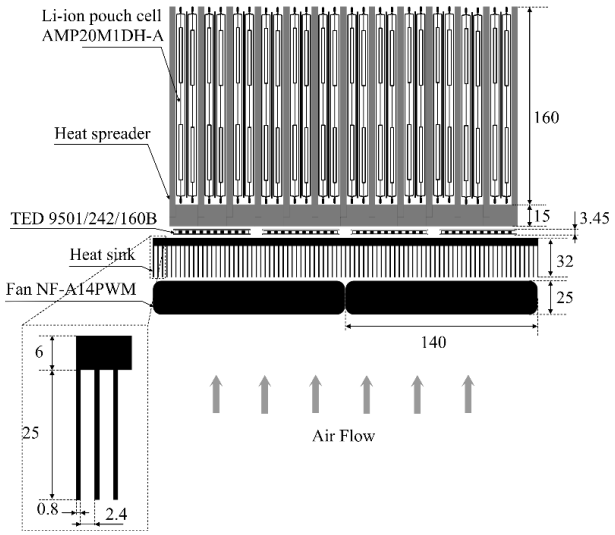

Fig. 6. BTMS assembly

C. BTMS modeling and simulation

Fig. 7 shows the thermal model of the proposed heat spreader. This model is obtained by exploring its symmetrical shape. The thermal resistances network include 1D resistances Θ_{D1} and Θ_{D2}, spreading resistance Θ_S and contact resistance Θ_C. The equivalent thermal resistance of the network Θ_{HSp} is expressed in (13). The spreading and the contact resistances were neglected due to their very small values as was suggested by Yovanovich [24]

$$\Theta_{HSp} = \left(t/4c + d/s\right)/K.L \tag{13}$$

With s, d and t being the dimensions shown in Fig. 7, L and K are the length and the thermal conductivity of the heat spreader respectively.

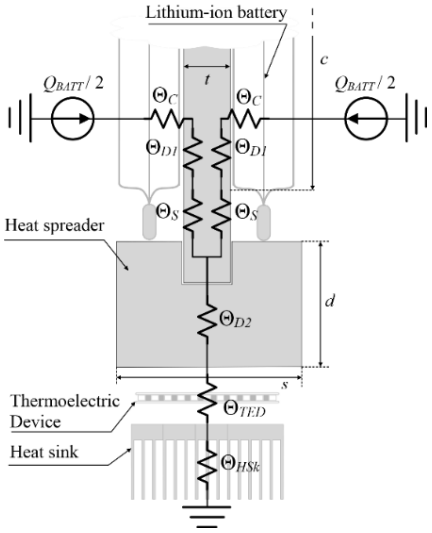

Fig. 7. Thermal network for the heat transfer between the li-ion battery cells, the heat spreader, TEDs and the heat sink.

The BTMS has two modes of operation, which are activated according to the quantity of heat generated by the li-ion batteries:

1. *Mode 1* – Passive mode: the generated heat is removed by the heat-spreader, TEDs (without applied power) and heat sinks, while applying power to fans only. This mode of operation works when the battery's temperature: –10°C<T_{BATT}<40°C
2. *Mode 2* – Active mode: the Peltier coolers and associated fans are turned on. The BTMS consumes power from the li-ion battery pack. This mode of operation is activated in case of extreme operation of the electric vehicle (high ambient temperature, high discharge current and/or defective battery cell). Active heating for T_{BATT} < –10°C and active cooling for T_{BATT}> 40°C.

D. Passive mode of operation

When no current is applied to the BTMS, it can be modeled using the resistance network shown in Fig. 8. The heat generated by the li-ion battery cells is removed through the heat spreaders, the TEDs and the heat sinks by natural conduction.

$$T_{BATT} = T_\infty + Q_{BATT}.\Theta_{Eq} \tag{14}$$

with

$$\Theta_{Eq} = \Theta_{B/H} + \Theta_{HSp} + \Theta_{H/T} + \Theta_{TED} + \Theta_{T/H} + \Theta_{HSk} \tag{15}$$

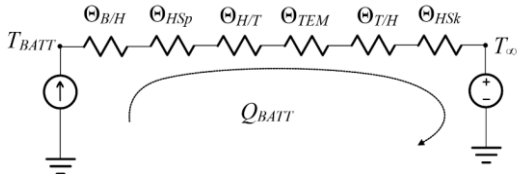

Fig.8. BTMS model in passive and shallow active modes

Fig. 9 shows 3D plot of (6). It shows a maximum battery temperature of 64 °C under extreme conditions of $T_\infty = 40$ °C and $Q_{BATT} = 105$ W.

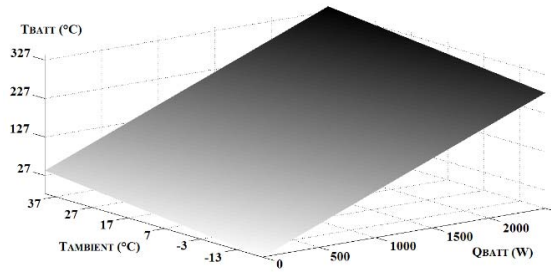

Fig. 9. 3D plot for (6) showing the battery's temperature T_{BATT} as function of the ambient temperature and the generated heat Q_{BATT}

E. Active mode of operation

When the thermoelectric coolers are turned on, the BTMS model becomes of Fig. 10.

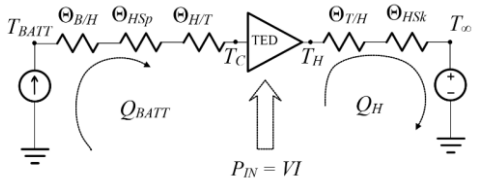

Fig.10. Thermal model of BTMS in active mode of operation

The heat transfer is plotted in Fig. 11. For high current values, it shows a limitation in heat removal capabilities due to joule effect made by TED's internal resistance. This Joule effect heating becomes more significant beyond an input current of 3A for each TEC module.

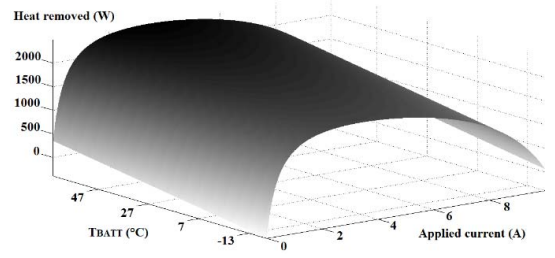

Fig. 11. 3D plot of the heat removed vs. the applied current and the ambient temperature.

V. Experimental Testing

The proposed BTMS was submitted to C/1, 3C and 5C discharge currents, and to ambient temperatures of –20, 0, 24 and 40 °C inside the climatic chamber. The surface temperature of the cells was recorded along with the parasitic power consumed by the BTMS in order to operate the TEDs and the fans. The battery manufacturer specifies temperature limits of –30 °C<T_{BATT}<60 °C, however, BTMS control circuit was designed to turn-on the TEDs when the cell's temperature falls outside the range of –10 °C<T_{BATT}<40 °C in order to achieve maximum performance and life.

The BTMS was tested with a continuous discharge current of C/1, while measuring the voltage and current consumed by the BTMS in order to evaluate the total energy consumed to maintain the cell's temperature within the –10 °C<T_{BATT}<40 °C limits. Figs 12, 13 and 14 show the temperature of the battery surface, and table V shows the experimental results. After recharging the battery cell at CC/CV, C/1 test was repeated for ambient temperatures of 0 °C, 25 °C and 40 °C. Finally, the same procedure was repeated for 3C and 5C for the same ambient temperature values.

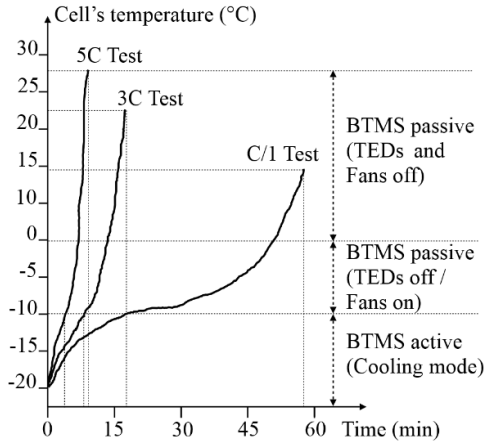

Fig. 12. –20 °C test results for C/1, 3C and 5C constant current discharge

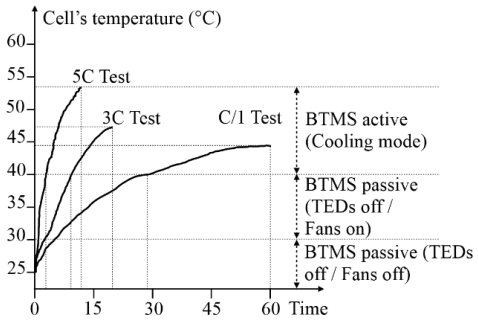

Fig. 13. 25 °C testing results

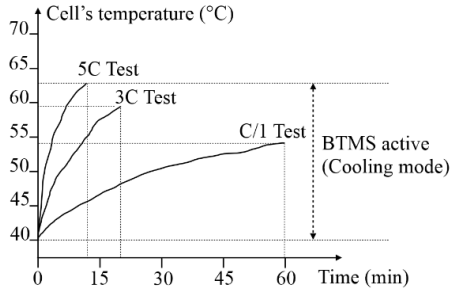

Fig. 14. 40 °C testing results

V. Results And Discussions

The BTMS maintains at all times the battery pack temperature within the limits, while consuming no more than 4.8% of the maximal stored energy in the pack. This consumed parasitic energy does not include the added weight of the BTMS components (heat spreader, TEDs, heat sink and fans) on mobile applications such as electric vehicle (EV). In addition, the BTMS added the volume of the li-ion battery pack by 120%. This additional volume contributed to the passive cooling capabilities of the BTMS, which was accomplished due to the heat spreader design. Table IV shows the added weight, volume and the consumed parasitic energy needed to operate the BTMS (for the worst case scenario of $T\infty = -40$ °C).

TABLE IV: BTMS SPECIFICATION FOR A PACK OF 24 LI-ION CELLS

	Battery pack w/o BTMS	**BTMS**	**Added charge**
Total weight	12 kg	21.8 Kg	+81.66%
Total volume	6843 cm^3	15028cm^3	+120%
Total energy stored	1560 Wh	1485	4.8% (–75 Wh)

The overall testing of the proposed BTMS show it applicability for high and low temperature environments and high discharge currents. It consumes a total energy of 75Wh under extreme conditions. However, it adds significant weight and volume to the battery pack.

VI. Conclusion

This paper proposed a battery thermal management system (BTMS) for prismatic lithium-ion battery cells. It is designed to extract 2.5 KW of heat losses produced by a battery pack made of 24 cells and working under extreme conditions, such as an ambient temperature of 40°C and a continuous discharge current of 5C. In such conditions, the BTMS consumed 4.8% of the available energy stored in the li-ion battery pack. In regular ambient temperature values (0 to 20 °C), the BTMS consumed no power and worked in passive mode only. In the other hand, the added weight and volume to the battery pack were significant (+81.66% increase in weight and +120% increase in volume).

References

[1] L. Lu, X. Han, J. Li, et al. "A review on the key issues for lithium-ion battery management in electric vehicles," *Journal of power sources*, 2013, vol. 226, p. 272-288.

[2] C. Alaoui, Z.M. Salameh, "A novel thermal management for electric and hybrid vehicles," *IEEE transactions on vehicular technology*, 54(2), pp.468-476. 2005.

[3] A. Barré, B. Deguilhem, S. Grolleau, M. Gérard, F. Suard, D. A. Riu, "Review on lithium-ion battery ageing mechanisms and estimations for automotive applications," *J. Power Sources* 2013, 241, 680–689.

[4] N. Omar, M.A. Monem, Y. Firouz, J. Salminen, J. Smekens, O. Hegazy, H. Gaulous, G. Mulder, P. Van den Bossche, T. Coosemans, et al. "Lithium iron phosphate based battery—Assessment of the aging parameters and development of cycle life model," *Appl. Energy* 2014, 113, 1575–1585.

[5] C. Alaoui, Z. M. Salameh, W. A. Lynch, "The depth of discharge on sealed lead acid electric vehicle batteries," *Proceedings of the IASTED International Conference*, November 8-10, 1999, Las Vegas, Nevada – USA.

[6] Q. Wang, P. Ping, X. Zhao, G. Chu, J. Sun, and C. Chen, "Thermal runaway caused fire and explosion of lithium ion battery," *Journal of power sources*, 208, pp.210-224, 2012.

[7] C. Alaoui and Z. M. Salameh, "Electric Vehicle Diagnostic and Rejuvenation System (EVDRS)," *International journal of power & energy systems* 27.2 (2007): 151.

[8] C. Alaoui and Ziyad M. Salameh, "A novel system-on-chip system for diagnostic & rejuvenation for electric & hybrid vehicles," *Power Electronics, Electrical Drives, Automation and Motion*, 2006. SPEEDAM 2006. International Symposium on. IEEE, 2006.

[9] C. Alaoui, "Modular energy efficient and solid-state Battery Thermal Management System," *Wireless Technologies, Embedded and Intelligent Systems* (WITS), 2017 International Conference on. IEEE, 2017.

[10] E. Deiss, A. Wokaun, J.L. Barras, C. Daul, and P. Dufek, "Average Voltage, Energy Density, and Specific Energy of Lithium-Ion Batteries Calculation Based on First Principles," *Journal of the Electrochemical Society*, 144(11), pp.3877-3881, 1997.

[11] C. Alaoui, Z.M. Salameh, and W.A. Lynch, "Sealed lead acid electric vehicle batteries: A performance comparison study," *International journal of power & energy systems*, 21(3), pp.174-179. 2001.

[12] D. Bernardi, E. Pawlikowski, and John Newman, "A general energy balance for battery systems," *Journal of the electrochemical society*, Vol. 132, Issue. 1, pp: 5-12, 1985.

[13] C. Alaoui, "Solid-state thermal management for lithium-ion EV batteries," *IEEE Transactions on Vehicular Technology* 62.1 (2013): 98-107.

[14] A. Ali, and C. Alaoui, "FPGA-based control of thermoelectric coolers for laser diode temperature regulation," *International Journal of Engineering Science and Technology*, 4(4), 2012.

[15] C. Alaoui, "Electric vehicle energy management system," *Ph.D. Thesis*, 2001.

[16] Y.-W. Chang, C. C. Chang, "Thermoelectric air-cooling module for electronic devices," *Applied Thermal Engineering* 29 (13) (2009) 2731–2737.

[17] C. Alaoui, "Testing and Simulation of Solid State Heating and Cooling," *International Journal of Engineering Science and Technology*, 3(2), pp.1636-1641, 2011.

[18] S. Chatterjee, P.K. Purkait, D. Garg, "Athermalization of infra-red camera of projectile weapons," *Applied Thermal Engineering* 29 (10) (2009) 2106–2112.

[19] R. Chein, G. Huang, “Thermoelectric cooler application in electronic cooling,” Applied Thermal Engineering 24 (14–15)(2004) 2207–2217.
[20] H.-S. Huang, Y.-C. Weng, “Thermoelectric water-cooling device applied to electronic equipment,” *International Communications in Heat and Mass Transfer* 37 (2) (2009) 140–146
[21] C. Alaoui, “Thermal management for energy storage s ystem forsmart grid,” *Journal of Energy Storage,* 2017, vol. 13, p. 313-324
[22] Website: “Ferrotec Thermoelectric Modules - Peltier Cooler Model 9501/242/160 B” https://thermal.ferrotec.com/products/peltier-thermoelectric-cooler-modules/high-power/9501_242_160-b/
[23] Lin, X., Perez, H.E., Siegel, J.B., Stefanopoulou, A.G., Li, Y., Anderson, R.D., Ding, Y. and Castanier, M.P., “Online parameterization of lumped thermal dynamics in cylindrical lithium ion batteries for core temperature estimation and health monitoring,” *IEEE Transactions on Control Systems Technology*, 21(5), pp.1745-1755, 2013.
[24] M. M. Yovanovich, Y. S. Muzychka, and J. R. Culham,“Spreading resistance of isoflux rectangles and strips on compound flux channels,” *Journal of Thermophysics and Heat Transfer*, 13(4), pp.495-500, 1999.